Analysis of responses of three-dimensional spiking oscillators to pulse-train input

Hidehiro Nakano and Toshimichi Saito

Department of Electronics, Electrical and Computer Engineering
Hosei University
3–7–2, Kajino-cho, Koganei-shi, Tokyo, 184–8584
JAPAN

Abstract: - This paper studies responses of three-dimensional (3-D) spiking oscillators to pulse-train input. The 3-D spiking oscillator consists of a linear subcircuit and a state-resetting switch. In order to analyze responses of the circuits, we introduce a mapping procedure based on a one-dimensional (1-D) return map. We then consider a simple 3-D spiking oscillator based on an RLC circuit. For equidistant and non-equidistant periodic pulse-train inputs, this simple circuit can exhibit rich responses including chaos. We analyze these responses numerically by using the 1-D return maps and their Lyapunov exponents.

Key-Words: - Nonautonomous system, pulse-train, mapping procedure, chaos, bifurcation, synchronization

1 Introduction

This paper studies responses of three-dimensional (3-D) spiking oscillators to pulse-train input. The 3-D spiking oscillator is a piecewise linear circuit consisting of a linear subcircuit and a state-resetting switch. First, we introduce the objective circuit model and a normal form of the circuit equation in order to extract essential parameters. In order to analyze responses of the circuits, we introduce a mapping procedure based on a one-dimensional (1-D) map focusing on the moment when the input arrives. If the input is an equidistant periodic pulse-train, the 1-D map can be return map. If the input is a non-equidistant periodic pulse-train, the circuit dynamics can be analyzed by a composite of different 1-D maps corresponding to different pulse-intervals. We then consider a simple 3-D spiking oscillator based on an RLC circuit. If the input does not present, the circuit exhibits an equilibrium or chaotic attractor. For equidistant and non-equidistant periodic pulse-train inputs, this simple circuit can exhibit rich responses including chaos. We analyze these responses numerically by using the 1-D return maps and their Lyapunov exponents.

In our previous literature, autonomous 3-D spiking oscillators have been studied [1]-[3]. They can exhibit rich chaotic and bifurcating phenomena. Coupling the 3-D spiking oscillators by impulsive signals, a pulse-coupled network (PCN) can be constructed. The PCN can exhibit interesting chaos synchronous phenomena. Note that 2-D spiking oscillators correspond to integrate-and-fire neurons (IFNs, [4]). PCNs of the IFNs can exhibit various synchronous and asynchronous phenomena [5][6], and have many applications including associative memories [7] and image processors [8].

This paper provides the basic analysis results for 3-D spiking oscillators having pulse-train input. Preliminary results can be found in Ref. [3]. These studies will be fundamental to engineering applications including PCNs, pulse-based communications [9][10] and time series prediction [11].

2 Circuit Model

Fig. 1 shows the circuit family of the spiking oscillators with the pulse-train input $U(t)$. Let the linear subcircuit N include one memory element characterized by a state variable z. The circuit dynamics is described by the following equation if the switch S is opened:

$$\frac{d}{dt}\begin{bmatrix} v \\ z \end{bmatrix} = \begin{bmatrix} a_{11} & a_{12} \\ a_{21} & a_{22} \end{bmatrix} \begin{bmatrix} v \\ z \end{bmatrix}, \tag{1}$$

where the parameters a_{11} to a_{22} are determined by the structure of N. $U(t)$ is the pulse-train input:

$$U(t) = \begin{cases} V_H & \text{at } t = 0 + \sum_{n=1}^{m} T_n, \\ V_L & \text{otherwise}, \end{cases} \tag{2}$$

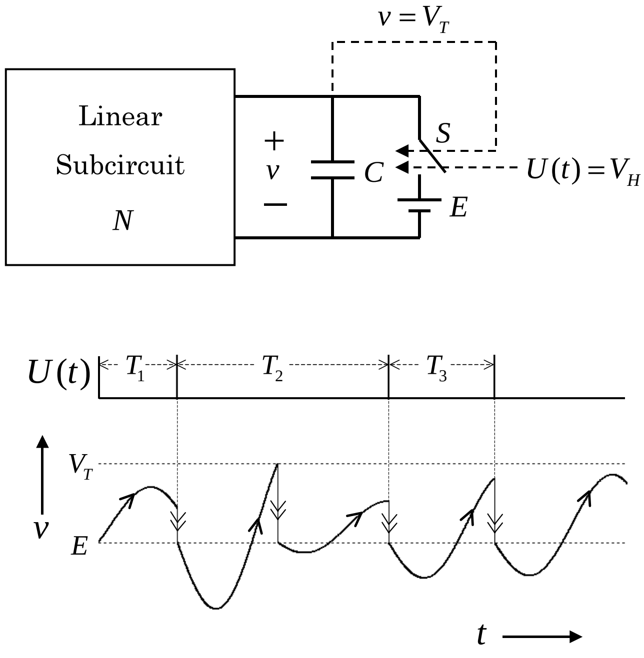

Fig. 1: A circuit family of spiking oscillators with pulse-train input.

where m is a positive integer, $V_H > V_L$, and $T_n > 0$ is the nth pulse-interval. The switch S is closed instantaneously if either v reaches the threshold V_T or the impulse signal $U(t) = V_H$ arrives. At the moment when S is closed, v is reset to the base voltage E instantaneously, holding z=constant. Hereafter the reset by $v(t) = V_T$ (respectively, $U(t) = V_H$) is referred to as self-switching (respectively, compulsory-switching). The dynamics of these switchings are described by

$$\begin{aligned}
&\text{self-switching: if } v(t) = V_T \text{ then}\\
&\quad (v(t^+), z(t^+)) = (E, z(t)),\\
&\text{compulsory-switching: if } U(t) = V_H \text{ then}\\
&\quad (v(t^+), z(t^+)) = (E, z(t)).
\end{aligned} \tag{3}$$

We focus on the case where Equation (1) has complex characteristic roots $\delta\omega \pm j\omega$, where

$$\delta\omega = \frac{a_{11} + a_{22}}{2},$$
$$\omega^2 = a_{11}a_{22} - a_{12}a_{21} - \left(\frac{a_{11} + a_{22}}{2}\right)^2 > 0.$$

In this case the state vector (v, z) can vibrate below the threshold V_T. Using the dimensionless variables and parameters:

$$\begin{aligned}
&\tau = \omega t,\ x = \frac{v}{V_T},\ y = \frac{1}{V_T}\left(p\,v + \frac{a_{12}}{\omega}\,z\right),\\
&u(\tau) = \frac{1}{V_H - V_L}\left(U\left(\tfrac{\tau}{\omega}\right) - V_L\right),\\
&p = \frac{a_{11} - a_{22}}{2\omega},\ q = \frac{E}{V_T},\ d_n = \omega T_n,
\end{aligned} \tag{4}$$

Equations (1), (2) and (3) are transformed into the following normal form equation:

$$\begin{aligned}
&\frac{d}{d\tau}\begin{bmatrix} x \\ y \end{bmatrix} = \begin{bmatrix} \delta & 1 \\ -1 & \delta \end{bmatrix}\begin{bmatrix} x \\ y \end{bmatrix},\\
&\text{for } x(\tau) < 1 \text{ and } u(\tau) = 0,\\
&u(\tau) = \begin{cases} 1 & \text{at } \tau = 0 + \sum_{n=1}^{m} d_n, \\ 0 & \text{otherwise}, \end{cases}\\
&\text{self-switching: if } x(\tau) = 1 \text{ then}\\
&\quad (x(\tau^+), y(\tau^+)) = (q, y(\tau) - p(1 - q)),\\
&\text{compulsory-switching: if } u(\tau) = 1 \text{ then}\\
&\quad (x(\tau^+), y(\tau^+)) = (q, y(\tau) - p(x(\tau) - q)).
\end{aligned} \tag{5}$$

Apart from the normalized pulse-intervals d_n, this normal form equation has three parameters: the damping δ, the jumping slope p, and the base level q. The exact piecewise solution for $x(\tau) < 1$ and $u(\tau) = 0$ is

$$\begin{bmatrix} x(\tau) \\ y(\tau) \end{bmatrix} = e^{\delta\tau}\begin{bmatrix} \cos\tau & \sin\tau \\ -\sin\tau & \cos\tau \end{bmatrix}\begin{bmatrix} x(0) \\ y(0) \end{bmatrix}, \tag{6}$$

where $(x(0), y(0))$ denotes an initial state vector at $\tau = 0$.

3 Mapping Procedure

In order to analyze responses of the circuit, we introduce a mapping procedure based on a 1-D map. Let the input $u(\tau)$ have the first and second impulses at $\tau = 0$ and $\tau = d$, respectively. Let $L_0 = \{\,(x, y, \tau)\,|\, x = q,\ \tau = 0\,\}$ and let $L_1 = \{\,(x, y, \tau)\,|\, x = q,\ \tau = d\,\}$. Since x is reset to q at every compulsory-switching moment, we can set the initial condition as $(x, y, \tau) \in L_0$ without loss of generality. Let points on L_0 and L_1 be represented by their y-coordinate. As a trajectory starts from a point $y_0 \in L_0$ at $\tau = 0$, the next compulsory-switching occurs at $\tau = d$ and the trajectory is reset to a point $y_1 \in L_1$. Then we can define the following 1-D map:

$$H_d:\ L_0 \to L_1, \quad y_0 \mapsto y_1, \quad y_1 = H_d(y_0), \tag{7}$$

where the subscript d corresponds to the pulse-interval d. For $0 < \tau < d$, some self-switchings may occur. However, focusing on the compulsory-switching moment, the dynamics can be analyzed by the 1-D map. This 1-D map is given analytically by using exact piecewise solutions [3].

The 1-D map (7) can be a return map if $d_n = d$ for all n. Let $DH_d(y_0) \equiv \frac{d}{dy_0}H_d(y_0)$. Then the Lyapunov exponent of the return map is given by

$$\lambda = \lim_{N\to\infty}\frac{1}{N}\sum_{n=0}^{N-1}\ln|DH_d(y_n)|. \tag{8}$$

For $m \geq 2$, the sequence $\{d_n\}$ is m periodic if there exists a positive minimum integer m such that $d_{n+m} = d_n$ for all n. Then the dynamics can be described by a composite of different 1-D maps H_{d_n} corresponding to different pulse-intervals d_n:

$$H : H_{d_m} \circ H_{d_{m-1}} \circ \cdots \circ H_{d_1}, \quad y_0 \mapsto y_m. \tag{9}$$

Since the sequence $\{d_n\}$ is m periodic, this composite map is a return map. The Lyapunov exponent of the return map is given by

$$\begin{aligned} \lambda &= \lim_{N\to\infty} \frac{1}{mN} \sum_{i=0}^{N-1} \ln |DH(y_{mi})| \\ &= \lim_{N\to\infty} \frac{1}{mN} \sum_{i=0}^{N-1} \sum_{j=1}^{m} \ln |DH_{d_j}(y_{mi+j-1})|. \end{aligned} \tag{10}$$

4 A Simple Circuit Model

Fig. 2 shows the simple 3-D spiking oscillator such that the linear subcircuit N in Fig. 1 is replaced with the RL subcircuit. Let the resistor R take both positive and negative value. If the switch S is opened, the circuit dynamics is described by

$$C\frac{dv}{dt} = i, \quad L\frac{di}{dt} = -v - Ri, \quad \text{for } v(t) < V_T \text{ and } U(t) = V_L. \tag{11}$$

The relationship between Equations (1) and (11) is the following:

$$z = i, \quad \begin{bmatrix} a_{11} & a_{12} \\ a_{21} & a_{22} \end{bmatrix} = \begin{bmatrix} 0 & 1/C \\ -1/L & -R/L \end{bmatrix}. \tag{12}$$

Using the dimensionless variables and parameters in (4), we obtain the normal form equation (5), where $p = -\delta$. That is, apart from the normalized pulse-intervals d_n, this circuit is characterized by two parameters: the damping δ and the base level q. The parameters

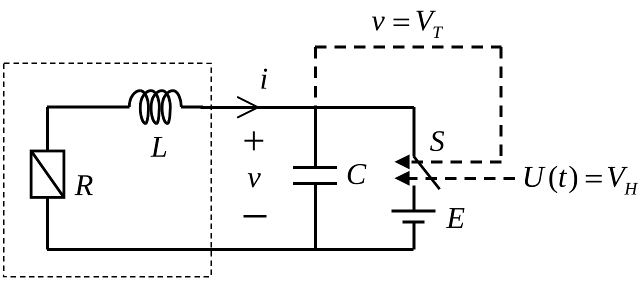

Fig. 2: A simple 3-D spiking oscillator with pulse-train input.

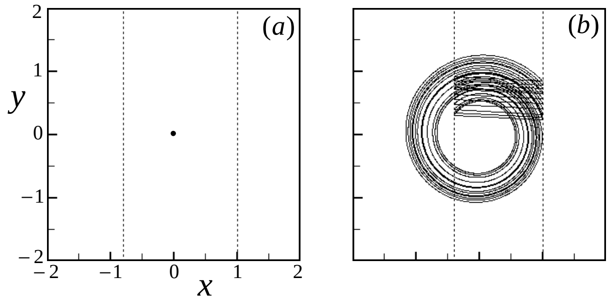

Fig. 3: Typical attractors without input. (a) Equilibrium attractor (the case A: $\delta = -0.01$, $q = -0.8$). (b) Chaotic attractor (the case B: $\delta = 0.05$, $q = -0.4$).

δ and q can be controlled easily by the values R and E, respectively. For simplicity, we focus (δ, q) on the following two cases:

$$\begin{aligned} \text{A}: &\quad \delta = -0.01, \quad q = -0.8 \\ \text{B}: &\quad \delta = 0.05, \quad\ \ q = -0.4 \end{aligned}$$

If the input is not present for the cases A and B, the circuit exhibits equilibrium and chaotic attractors as shown in Fig. 3(a) and (b), respectively. Theoretical parameters condition for existence of each attractor can be found in Refs. [2] and [3]. Hereafter, we investigate responses to periodic pulse-train input such that $d_n = d_A$ for odd n and $d_n = d_B$ for even n.

4.1 Typical responses in the case A

We consider how the input $u(\tau)$ change the equilibrium attractor in Fig. 3(a). Fig. 4 shows typical responses to periodic pulse-train inputs and corresponding 1-D return maps with the Lyapunov exponents. Fig. 4(a) shows the chaotic response to equidistant periodic pulse-train input ($d \equiv d_A = d_B$). This chaotic response can be confirmed by a positive Lyapunov exponent of the 1-D return map in Fig. 4(e). For chaos generation, local unstability is required. The circuit can exhibit self-switching by the occurrence of compulsory-switching. These switchings can change the equilibrium attractor in Fig. 3(a) into the chaotic attractor. Figs. 4(b) and (c) show coexistence of the periodic and chaotic responses to equidistant periodic pulse-train input. The circuit exhibits either response depending on the initial state. This coexistence phenomenon can also be confirmed in the 1-D return map in Fig. 4(f). Fig. 4(d) shows the periodic response to non-equidistant periodic pulse-train input ($d_A \neq d_B$). The corresponding 1-D return map in Fig. 4(g) is a composite map of the chaotic 1-D map in Fig. 4(e) and the coexistence 1-D map in Fig. 4(f). A stable fixed point y_p corresponding to the periodic response appears in the composite map. Fig. 6(a) shows the bifurcation diagram for d_A and d_B.

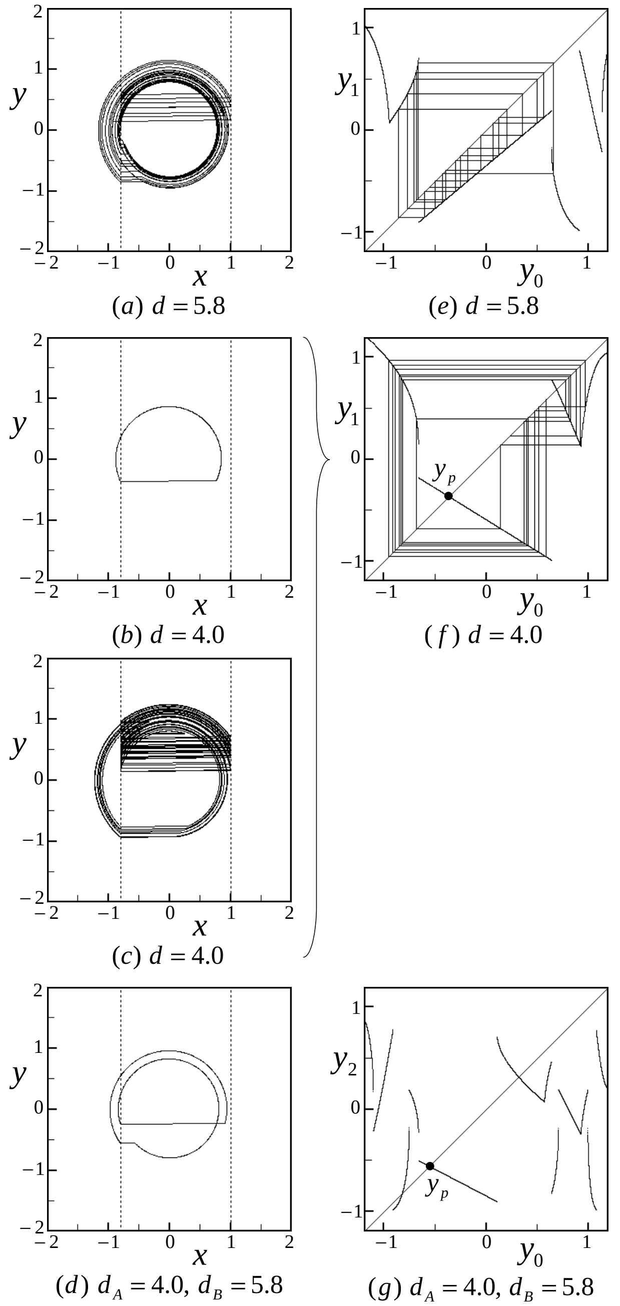

Fig. 4: Typical responses and 1-D return maps for periodic pulse-train input (the case A: $\delta = -0.01$, $q = -0.8$). (a) Chaotic response. (b) and (c): Coexistence of periodic and chaotic responses. (d) Periodic response. (e) 1-D return map $y_1 = f_d(y_0)$ ($\lambda = 0.0479$). (f) 1-D return map $y_1 = f_d(y_0)$ ($\lambda = -0.477$ for periodic attractor; $\lambda = 0.427$ for chaotic attractor). (g) Composite return map $y_2 = f_{d_A} \circ f_{d_B}(y_0)$ ($\lambda = -0.326$).

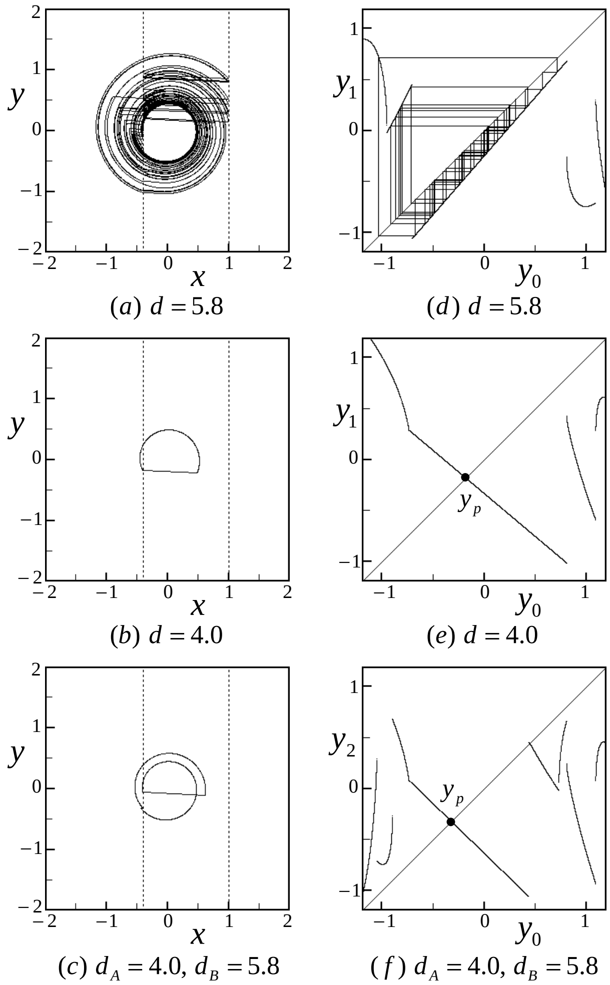

Fig. 5: Typical responses and 1-D return maps for periodic pulse-train input (the case B: $\delta = 0.05$, $q = -0.4$). (a) Chaotic response. (b) Periodic response. (c) Periodic response. (d) 1-D return map $y_1 = f_d(y_0)$ ($\lambda = 0.276$). (e) 1-D return map $y_1 = f_d(y_0)$ ($\lambda = -0.169$). (f) Composite return map $y_2 = f_{d_B} \circ f_{d_A}(y_0)$ ($\lambda = -0.0135$).

4.2 Typical responses in the case B

We consider how the input $u(\tau)$ change the chaotic attractor in Fig. 3(b). Fig. 5 shows typical responses to periodic pulse-train inputs and corresponding 1-D return maps with the Lyapunov exponents. Fig. 5(a) shows the chaotic response to equidistant periodic pulse-train input ($d \equiv d_A = d_B$). This chaotic response can be confirmed by a positive Lyapunov exponent of the 1-D return map in Fig. 5(d). Fig. 5(b) shows the periodic response to equidistant periodic pulse-train input. A stable fixed point y_p corresponding to the periodic response appears in the 1-D return map 5(e). This means that the periodic pulse-train input changes the chaotic attractor in Fig. 3(b) into the periodic attractor. Fig. 5(c) shows the periodic response to non-equidistant periodic pulse-train input ($d_A \neq d_B$). The corresponding 1-D return map in Fig. 5(f) is a composite map of the chaotic 1-D map in Fig. 5(d) and the periodic 1-D map in Fig. 5(e). A stable fixed point y_p corresponding to the periodic response appears in the composite map. Fig. 6(b) shows the bifurcation diagram for d_A and d_B.

5 Conclusions

We have studied 3-D spiking oscillators with pulse-train input. As an analysis tool, we have proposed a mapping procedure based on a 1-D map focusing on the moment of compulsory-switching. We have presented a simple 3-D spiking oscillator based on an RLC circuit. Applying equidistant and non-equidistant periodic pulse-train inputs, the circuit can exhibit various chaotic and periodic responses. Using the mapping procedure, we have analyzed these responses.

In future works, we are considering (1) detailed analysis of bifurcation phenomena for wider parameter region, and (2) analysis of responses of circuits to non-periodic (or chaotic) pulse-train input.

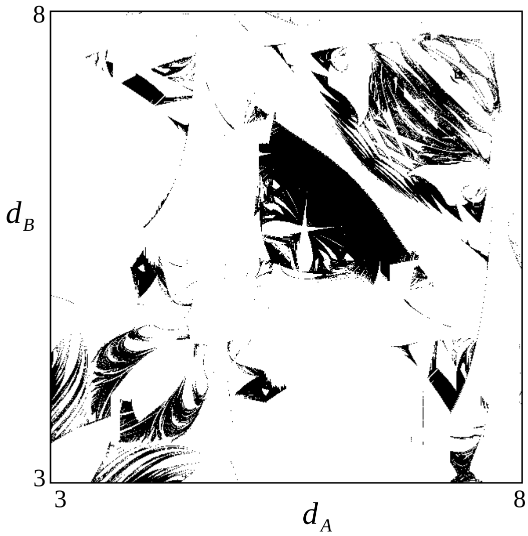

(a) The case A: $\delta = -0.01$, $q = -0.8$

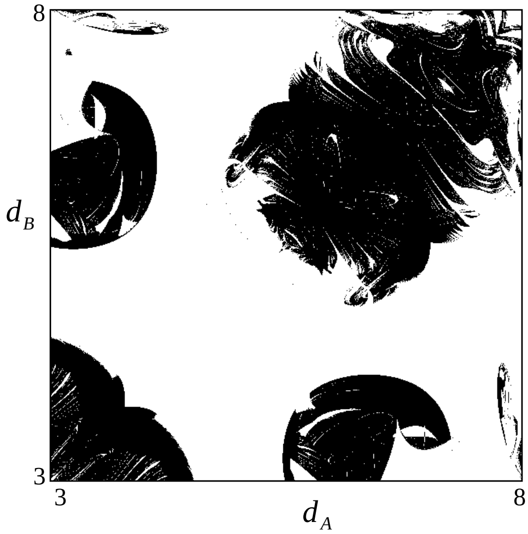

(b) The case B: $\delta = 0.05$, $q = -0.4$

Fig. 6: Bifurcation diagrams. In the black and white parts, the Lyapunov exponents of return maps have positive and negative values, respectively.

References:

[1] K. Mitsubori and T. Saito, "Mutually pulse-coupled chaotic circuits by using dependent switched capacitors," *IEEE Trans. Circuits Systs. I*, vol. 47, no. 10, pp. 1469-1478, 2000.

[2] H. Nakano and T. Saito, "Basic dynamics from a pulse-coupled network of autonomous integrate-and-fire chaotic circuits," *IEEE Trans. Neural Networks*, vol. 13, no. 1, pp. 92-100, 2002.

[3] K. Miyachi, H. Nakano and T. Saito, "Response of a simple dependent switched capacitor circuit to a pulse-train input," *IEEE Trans. Circuits Systs. I*, vol. 50, no. 9, pp. 1180-1187, 2003.

[4] J. P. Keener and F. C. Hoppensteadt and J. Rinzel, "Integrate-and-fire models of nerve membrane response to oscillatory input," *SIAM J. Appl. Math.*, vol. 41, pp. 503-517, 1981.

[5] R. E. Mirollo and S. H. Strogatz, "Synchronization of pulse-coupled biological oscillators," *SIAM J. Appl. Math.*, vol. 50, pp. 1645-1662, 1990.

[6] E. Catsigeras and R. Budelli, "Limit cycles of a bineuronal network model," *Physica D*, vol. 56, pp. 235-252, 1992.

[7] E. M. Izhikevich, "Weakly pulse-coupled oscillators, FM interactions, synchronization, and oscillatory associative memory," *IEEE Trans. Neural Networks*, vol. 10, no. 3, pp. 508-526, 1999.

[8] S. R. Campbell, D. Wang and C. Jayaprakash, "Synchrony and desynchrony in integrate-and-fire oscillators," *Neural Comput.*, vol. 11, pp. 1595-1619, 1999.

[9] T. Stojanovsky, L. Kocarev, and U. Parlitz, "Driving and synchronizing by chaotic impulses," *Phys. Rev. E*, vol. 54, pp. 2128-2131, 1996.

[10] M. Sushchik, N. Rulkov, L. Larson, L. Tsimring, H. Abarbanel, K. Yao and A. Volkovskii, "Chaotic pulse position modulation: A robust method of communicating with chaos," *IEEE Commun. Lett.*, vol. 4, no. 4, pp. 128-130, 2000.

[11] Y. Kanno and T. Ikeguchi, "Prediction on nonlinear time series of amplitude and event information," *Proc. NOLTA*, vol. 1, pp. 275-278, 2001.